Towards Forming Optimal Communication Network for Effective Power System Restoration

Volkova, A., Ghasemi, A. & de Meer, H.

Original citation & hyperlink:
Volkova, A, Ghasemi, A & de Meer, H 2024, 'Towards Forming Optimal Communication Network for Effective Power System Restoration', IEEE Transactions on Network and Service Management, vol. 21, no. 5, pp. 5250-5259.
https://dx.doi.org/10.1109/TNSM.2024.3429204

DOI 10.1109/TNSM.2024.3429204
ISSN 1932-4537

Publisher: Institute of Electrical and Electronics Engineers

Towards Forming Optimal Communication Network for Effective Power System Restoration

Anna Volkova, Abdorasoul Ghasemi, and Hermann de Meer

***Abstract*—Restoration of modern interdependent Information and Communication Technology (ICT) and power networks relies on preplanned and reactive strategies to consider simultaneous communication and power system recovery. This paper addresses the problem of finding and energizing a proper communication network connecting the distributed power grid assets in the restoration process, assuming a probability of infeasibility of recovering each communication node. The proper network has the minimum size, meets the communication requirements of power system recovery, and guarantees robustness against ICT nodes not being recoverable during restoration. The problem is formulated as a multi-objective optimization problem and solved using the genetic algorithm to find the optimal subgraph that ensures enough node-disjoint paths between the communicating power grid assets. Simulation results for the restoration strategy of the communication network associated with a power network are provided and discussed. The results show that networks' ability to mitigate the adverse consequences of node failures can be significantly improved by incorporating just a few additional nodes and links while keeping the ICT network compact and feasible for restoration.**

***Index Terms*—Cyber-physical energy system, robustness, power system restoration, communication network restoration**

I. Introduction

THE core objective of modern power systems is an uninterruptable supply of ever-increasing demand. However, the growing complexity of the interconnected ICT and power system, driven by digitalization and increasing share of renewable energy sources, can impact the stability of the power supply. Unanticipated worst-case circumstances, such as natural disasters, further exacerbate these challenges and can lead to wide-area outages. In the case of a blackout, power system restoration methods are applied to quickly and robustly restore the system back to its operational state [1].

Robust restoration procedures should be in place for volatile grids with a significant portion of renewable generators [1]. For this, bottom-up restoration methods are proposed to gradually restore the grid by employing grid-forming inverter-interfaced grid assets, e.g., renewable generators, battery storage systems, to form self-contained grid islands at medium [2] and low voltage [3] grid levels. Robustness, defined as the trustworthiness of a system in the face of challenges [4], is a key concern for the interconnected ICT and power system restoration. A high level of interdependency between two systems can be beneficial, e.g., increased observability of the available grid assets during the restoration, and disadvantageous, e.g., reduced robustness against cascading failures [5]. The lack of robustness in the grid restoration process may result in ineffective restoration of the loads or, in the worst case, rollback to the blackout state.

The known bottom-up restoration methods continuously rely on ICT to enable correct and reliable status and control message exchange between the geographically dispersed grid components. However, most of those methods do not consider the impact of ICT system disruption, which restricts the designed communication procedures [6], [7]. As a result, power system restoration methods assume that normal or degraded [8] communication between the power grid nodes is possible during the whole restoration period. This does not always hold in real-world situations since the ICT components may be disrupted or lack both primary (from the grid) and emergency (from an installed battery) power supply. The power system restoration process should identify and prioritize which ICT loads should be restored [2]. A correct and robust strategy for ICT energization is crucial to ensure that all necessary power grid assets can communicate effectively.

In this work, ICT network restoration is defined as a process of finding a subnetwork to be energized to enable communication between all required power grid assets during the power system restoration. Since the availability of the ICT nodes during an emergency cannot be known in advance, ICT network restoration should be performed in parallel to the power system restoration process after the blackout happened. The problem of power system restoration is already complex due to its multi-objective nature and power grid constraints [2]. Additional, often conflicting, ICT restoration objectives, such as maximizing network performance and robustness, result in even higher complexity. Therefore, the problem of ICT network restoration can be solved separately and injected into power grid restoration decision-making. This can be done by indicating necessary ICT nodes as priority loads in input to the power system restoration.

This paper discusses the problem of finding the optimal ICT network for power system restoration. The core objective of such a communication network is to connect all the power system nodes concerning their communication requirements. At the same time, in challenging conditions of the power system restoration, ICT network restoration should not force the power system to energize insignificant power buses to pick up more ICT loads. Therefore, the size of the ICT network should be kept small while proving the best possible service. Furthermore, there is no guarantee that an ICT node is not damaged and can be actually recovered during the restoration.

Anna Volkova and Hermann de Meer are with the University of Passau, Passau, Germany. Email: (anna.volkova, hermann.demeer).uni-passau.de.

Abdorasoul Ghasemi is with the Research Centre for Computational Science and Mathematical Modelling, Coventry University, Coventry, UK, Email: ae4959@coventry.ac.uk

Hence, the proposed ICT network should guarantee robustness against such failures.

This study proposes a methodology for ICT network restoration concerning conflicting objectives and provides the following contributions:

- The paper introduces a graph-theoretical approach to derive a realistic model of the interconnected ICT and power system. The model comprises the medium voltage level of the power grid and the access and backhaul level of the ICT networks while capturing the interdependencies between the ICT and power system and within ICT system.
- The problem of finding an optimal ICT network for power system restoration is formulated as a multi-objective optimization problem. On the one hand, the solution network should have a minimum size to avoid additional restoration efforts. On the other hand, the solution network should be robust against target ICT nodes being unrecoverable. To guarantee that the solution network can accommodate all communication demands, the multi-commodity flow problem is introduced as an additional constraint.
- A Genetic Algorithm (GA)-based approach is utilized to solve the formulated problem since it can handle graph structures flexibly and address different objectives. The method's capability to consider different formulations of the objectives is demonstrated. The robustness of the solutions is extensively tested for the varying probability of ICT nodes to be not recoverable.

In the following, Section II provides an overview of the related work. Section III introduces the interconnected system and the modeling approach. Section IV presents problem formulation and describes the methodology. Section V presents the obtained results and discusses the core insights. Finally, the paper is concluded in Section VI.

II. Related Work

The problem of ICT network restoration for the power distribution grid restoration has not been extensively studied in the literature. Several distributed optimization-based power system restoration methods have considered some level of ICT impairment and improved robustness of information exchange within the algorithm [8], [9]. However, these methods do not consider ICT restoration, namely, finding a strategy for an ICT network to be energized alongside the power system restoration.

At the same time, the problem of ICT system restoration after a disastrous event has been formulated independently from the power system restoration with many different objectives. It has been primarily expressed as a problem of finding the best schedule of repair interventions to increase available network capacity. In [10], the communication network recovery after a massive failure is aimed to optimize throughput through a schedule of repair interventions under a limited resource budget and with complete knowledge regarding the damage locations. The method described in [10] provides an early insight into the ICT restoration process. Still, it is only applicable when the location of the damaged ICT components is detected, and the operator can proceed with repairs. In our work, in contrast, an ICT network is formed based on the available infrastructure without full knowledge of the node failures and time budget to repair the components. The formed ICT network is fed as input to the power grid restoration algorithm, which aims to energize these ICT loads. The schedule-based repair method, described in [10], may be applied as the next step to restore the unrecoverable ICT nodes.

In [11], communication network recovery after a massive failure has been performed to establish communication for mission-critical services, including communication between power plants. A mixed integer linear programming problem is formulated to obtain a recovery schedule for a disrupted network. In the modeling approach of [11], a node metric is introduced to identify the profit value of the particular ICT node to indicate its priority to be recovered. The method is focused on the optimal flow distribution and considers node repair and establishment of new links and nodes. The authors in [12] aim to restore critical services after large-scale failures and perform progressive network recovery under uncertain knowledge regarding the location of damages to minimize the total repair cost. The method returns a recovery schedule that satisfies the critical demand flows while minimizing the proposed expected recovery cost function under network capacity constraints. The solution uses an iterative stochastic recovery algorithm to meet communication demands between the critical services. Both methods focus on scheduling the repair interventions. This process is time-consuming and, therefore, not applicable for bottom-up restoration, in which the resources of the existing ICT network should be used to build up the island grids right after the blackout.

In [13], the ICT system restoration is studied in relation to the interconnected ICT and power system. The authors discuss cascading failures mitigation and recovery of the interconnected ICT core and power transmission networks. The problem of power grid recovery is formulated as an instance of the knapsack problem. The ICT network is considered as a source of knowledge regarding the failures of the controllable power grid components. Our work focuses on ICT system recovery for the power distribution grid, considers access and backhaul ICT network levels, treats power system restoration as a black box, and provides more detailed modeling of the interconnected system based on scenarios retrieved from the open data. Our work also focuses on proving a robust ICT network right after the blackout based on the available infrastructure.

III. System Model and Assumptions

This section discusses the scenario, properties of the interconnected system, and the related assumptions. The presented modeling approach enables granular representation of the interconnected ICT and power system, considering the structure of the edge communication network.

A. Assumptions

The following scenario is assumed for the Meduim Voltage (MV) power grid with a high share of the renewable grid-

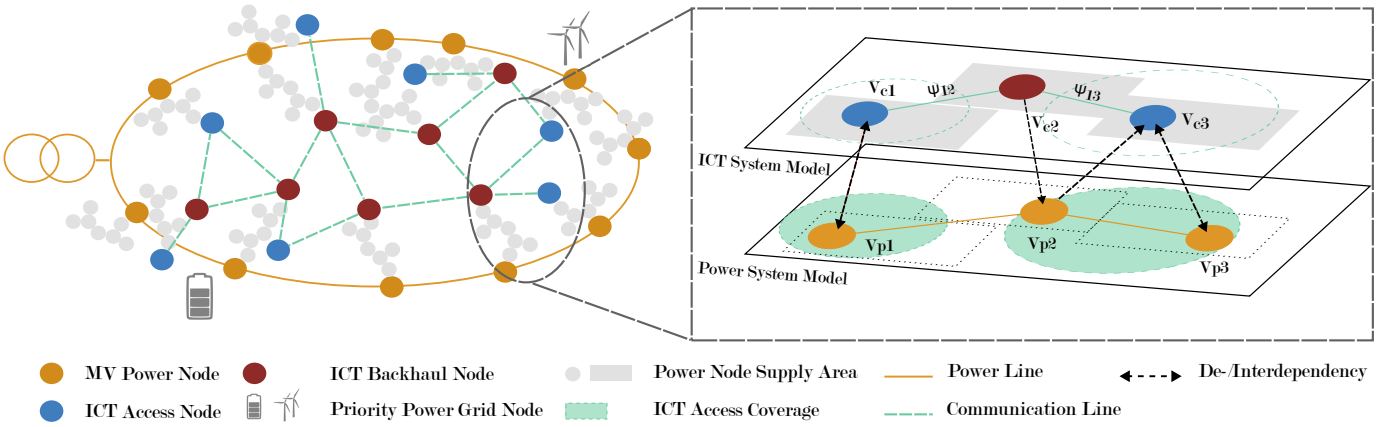

Fig. 1. On the left: The overall system scenario, which demonstrates the spatial relationship between medium voltage grid, access, and backhaul ICT nodes. On the right: Magnified interconnected ICT and power system model, which includes power grid and ICT levels. The inter-level edges capture dependency types between power and ICT nodes based on the relations between the ICT node coverage and the power bus supply area.

forming inverter-interfaced generators. A disastrous event has led to the wide-area outage of both ICT and the power system, including potential equipment damage, and service interruption in both systems. Immediately following this outage, the MV grid is to be restored in a bottom-up manner. This restoration uses grid-forming inverter-interfaced renewable generators and battery storage systems capabilities to form self-contained grid islands [14]. While for the formation and control of the smaller island grids at a low voltage level, local communication between power-electronic devices may be sufficient [15], forming and synchronization of multiple larger grid islands requires an exchange of data over a communication network [16], [17]. Distributed optimization algorithms are often proposed to derive the best schedule for load pick-up during the bottom-up restoration. They use ICT system to gather information and distribute the solution over MV grid nodes with installed controllers [2]. Hence, the model's core is the topology of the MV grid and its corresponding supply area. Figure 1 describes the scenario and demonstrates the MV grid nodes (buses) and respective supply areas. The MV power grid is an open ring network according to observations in [18]. Some grid nodes have attached large generation sites or battery storage, making those more crucial in the restoration process.

The ICT system is assumed to start from the blackout state. The ICT nodes next to important power grid nodes are supported by the emergency power supply or can be picked up by the grid-forming unit as part of the initial island. The rest of ICT nodes should be picked up during the restoration alongside the respective power buses. Some nodes may be disrupted and, therefore, not recoverable. This work assumes complete knowledge of the topology of both systems. This assumption is valid since the power system operators have information regarding the power grid topology and supporting ICT infrastructure. At the same time, no knowledge regarding whether an ICT node is recoverable is available before the start of the restoration process.

This work considers the public cellular network infrastructure. These networks have become more prominent for power distribution grid communication, especially with the ongoing digitalization of the medium and low voltage grid and the allocation of dedicated spectrum for critical infrastructures in many countries [19]. The cellular network comprises access nodes (base stations), backhaul nodes, and packet core nodes. Access nodes aggregate traffic transmitted from measurement devices installed on the power grid components. The backhaul nodes route the traffic toward the packet core in a multi-hop point-to-point manner. With the rapid development of cellular networks towards 5G, it can be assumed that access and backhaul nodes have intelligent features sufficient for enabling basic routing operations within their network segment. The developed methodology focuses on access and backhaul nodes to emphasize the role of regional edge ICT network structure in power distribution grid restoration. Access nodes (blue), their coverage areas as well as backhaul nodes (red) are presented in Figure 1. These ICT nodes are connected as loads at the grid supply area, marked in Figure 1.

B. Interconnected System Model

The scenario described in Section III-A is modeled in this section. The terms "bus" and "line" refer to power system infrastructure, while "node" and "link" refer to ICT system infrastructure. The interconnected model is presented on the right side of Figure 1. The power grid at MV is modeled as a graph $G_p = (V_p, E_p)$, where V_p is a set of n power system buses and E_p is a set of power lines. Each bus V_{p_a} has a weight σ_a with respect to its type, capacity and controllability. The ICT system is defined as a node- and edge-weighted graph $G_c = (V_c, E_c)$, where V_c is a set of k ICT nodes and E_c is a set of edges. This work focuses on cellular networks and assumes a cell as a circle. ICT node V_{c_i} has two weights: range r_i and coverage $Cov_i = \pi r_i^2$. As discussed in Section III-A, ICT system includes backhaul and access nodes. If V_{c_i} is a backhaul node, it only serves for forwarding packets collected by access nodes from the power buses in a point-to-point manner, and therefore, its range and coverage parameters are zero. Each edge in E_c has a weight ψ, representing the communication link's capacity.

The geospatial approach allows the modeling of the interconnected system concerning the present interdependencies.

The power supply dependency between ICT and power system nodes can be derived based on the supply area size A_a, which is as a geographic area supplied by the bus V_{p_a}. Cell coverage parameter Cov_i can be used to define if ICT node V_{c_i} is an access node for bus V_{p_a}, and therefore bus V_{p_a} is dependent on ICT node V_{c_i}. This allows introducing an additional ICT node weight ω_i, that represents the number of buses in the coverage Cov_i of the communication node V_{c_i}.

The size and composition of power and ICT network are important inputs to the methodology discussed in this work. However, the information regarding the amount of the power and ICT system nodes for an exemplary region is not disclosed to the public. Power grid models [18], [20] focus on the power system characteristics and do not represent real geographic scenarios. No realistic models are available for the public cellular ICT networks [21]. An access and backhaul network benchmark has been presented in [22]. However, the underlying geographical scenario is not detailed, and, therefore, ICT node density cannot be estimated. The approximate values for parameters of the system are discussed in [21]. The calculated density of medium voltage substations per 10 km^2 is 10 for urban and 5 for rural areas. The density of access nodes per 10 km^2 is 1.03 nodes for rural and 13.22 for urban areas. The average number of medium voltage substations in the coverage of an access node is 8 in rural and 56 in urban regions.

The interconnected ICT and power system model can be used to describe the overall system restoration process. The ICT node is picked up if it belongs to the supply area A_a of the respective energized bus V_{p_a}. ICT node coverage defines buses capable of communicating if the ICT node is picked up.

This work aims to form an optimal ICT network that covers all geographically scattered buses. The model of such a network can be derived from the interconnected system model discussed above. A graph $H = (V_h, E_h)$ is an undirected connected node-weighted and edge-weighted graph constructed from power system graph G_p and ICT system graph G_c. Nodes $V_h \in H$ are nodes of G_c with node weights ω expressing the number of underlying dependent power system buses within a coverage of ICT node. Each edge in E_h is defined by its capacity ψ_{ij}. The resulting graph is presented in Figure 2.

This representation reduces the complexity of the overall interconnected system model while accurately capturing power-ICT and intra-ICT interdependencies. Furthermore, the resulting model exhibits a realistic spatial scenario and is scalable to any region of the power distribution grid that uses cellular ICT networks.

IV. Problem Formulation and Solving Strategy

This section discusses problem formulation and the GA-based method, which effectively solves the formulated problem by considering all objectives and constraints. GA procedure, fitness function, and parameters are presented.

A. Problem Formulation

An optimal ICT network for the power system restoration is a subgraph H_{rest} of the graph H, which includes all the access nodes $\forall V_h \in H : \omega_{V_h} > 0$ and is routable concerning

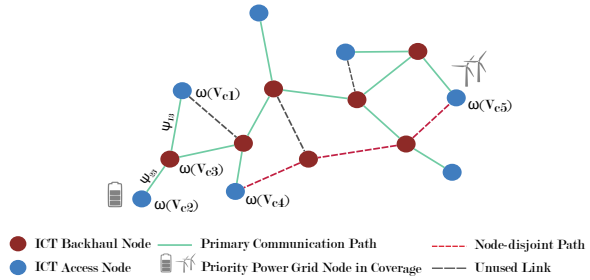

Fig. 2. ICT network model with attached dependent buses as node weights.

all communication demands from power buses attached at the access nodes. As discussed in Section III-A, power buses require communication in a many-to-many pattern, forming a multicast group.

One of the objectives of forming an ICT network for power system restoration is to reduce network size to avoid picking up low-impact power buses. However, a minimum-size tree network structure is insufficient in the challenging environment of the power system restoration. Such a structure does not provide robustness when an intermediate ICT node cannot be recovered, resulting in the overall network's inability to converge. An example of such a network is presented by the primary communication path in Figure 2, which connects all the access nodes.

To overcome this limitation, the communication between the access nodes should be diversified by introducing additional Node-disjoint Paths (NDPs), which only share their sources and destination nodes [23]. In Figure 2, a NDP is demonstrated between nodes V_{c_4} and V_{c_5}. Thus, an optimal ICT network is a minimal size subgraph H_{rest} of the graph H, which includes all the access nodes with the highest possible share of NDPs between them.

Let $x \in \mathbf{X}$ be a binary decision variable for edge e_{ij} from H to be included in subgraph $H_{rest} \in H$. Let $c(x)$ be a cost function of including an edge $e_{ij} \in H$ in H_{rest} according to Eq. (1). Let NDP_H be a number of NDPs in H, while $\text{NDP}_{H_{rest}}$ is the number of NDPs in H_{rest} for the given X. Let $g(\mathbf{X})$ be a function that assigns a penalty for a candidate subgraph based on the difference between NDP_H and $\text{NDP}_{H_{rest}}$ according to Eq. (2). The number of NDPs for each node can be set up according to the demanded level of robustness.

$$c(x) = \begin{cases} 1, & \text{if } e_{ij} \in H_{rest} \\ 0, & \text{if } e_{ij} \notin H_{rest} \end{cases} \tag{1}$$

$$g(\mathbf{X}) = 1 - \frac{NDP_{H_{rest}}}{NDP_H}, |V_H : \omega_{V_H} > 0| \geq 2 \tag{2}$$

A Multi-Commodity Flow (MCF) calculation is used to evaluate if a graph can accommodate all communication demands from power buses attached to the access nodes. The message between each source-destination pair of access nodes is a communication demand (commodity) to be forwarded. Each commodity k_i is defined by its source node s_i, destination node t_i, and size v_i: $k_i = (s_i, t_i, v_i)$. The amount of commodity at the access node equals its node weight ω.

A MCF consists of flow functions f_{ij}^i on the edges $e_{ij} \in H_{rest}$ for every commodity $k_i \in K$, that represent the flow of commodity k_i on this edge. Each edge e_{ij} is assigned with a link capacity parameter ψ_{ij} and the cost parameter d_{ij}. The cost d_{ij} of an edge equals the queuing delay experienced on this edge, according to Eq. (3). A problem of finding an assignment of flow variables for all flows with minimal total cost is called MCF problem [24]. Eq. (4) determines the range of flow variables.

$$d_{ij} = \frac{1}{\psi_{ij} - \sum_{i=1}^{K} f_{ij}^i}, \forall i, j \in H_{rest} \tag{3}$$

$$0 \leq f_{ij}^k \leq 1, \forall k \in K, \forall i, j \in H_{rest} \tag{4}$$

The information exchange between two pairs of buses is bidirectional, since the restoration optimization algorithms may require an exchange of the partial solutions [2]. While transferring the flow over the edge e_{ij}, no edge capacity ψ_{ij} should be violated according to the capacity constraint in Eq. (5). For every commodity k_i and every node in H_{rest}, a flow conservation rule is applied according to Eq. (6). Flow conservation controls that flow leaving the node equals the amount of flow entering the node. The flow is positive for source nodes s and negative for destination nodes t.

$$\forall i, j \in H_{rest} : \sum_{i=1}^{K} f_{ij}^i \leq \psi_{ij} \tag{5}$$

$$\sum_{(i,j)\in H_{rest}} f_{ij}^k - \sum_{(j,i)\in H_{rest}} f_{ji}^k = \begin{cases} f^k, & \text{if } i = s_i \\ -f^k, & \text{if } i = t_i, \forall i \in K \\ 0, & i \neq s_i,\ i \neq t_i \end{cases} \tag{6}$$

MCF calculation is used to ensure that the resulting graph H_{rest} is routable, what means MCF problem is feasible for the given candidate graph. One should note that minimization of the delay value can be considered as an additional objective to improve the quality of service of the solution network. In this work, the focus lies on size and robustness objectives.

Overall, the problem of finding ICT network for the power system restoration (Eq. (7)) is a problem of finding a subgraph H_{rest} of the graph H, that minimizes cost and penalty functions, while ensuring that all the access nodes are included, the H_{rest} is connected and MCF problem is feasible for H_{rest}.

$$\begin{aligned} &\underset{x_{ij}\in\mathbf{X}}{\text{minimize}} \quad \sum c_{ij} \cdot x_{ij}, \quad \underset{\mathbf{X}}{\text{minimize}} \quad g(\mathbf{X}) \\ &\text{subject to:} \\ &\forall V_H : \omega_{V_H} > 0, V_H \in H_{rest}, \\ &H_{rest} \text{ is connected,} \\ &\text{MCF is } \textit{feasible} \text{ w.r.t. Eq. (3), (4), (5), (6).} \end{aligned} \tag{7}$$

B. Overall Solution Approach

This work uses the meta-heuristic approach to solve the multi-objective constrained subgraph search problem discussed in Section IV-A. Meta-heuristic algorithms are designed to quickly and efficiently find passable, but not always optimal, solutions and are more adjustable considering additional problem variables and objectives. In this regard, GAs provide sufficient flexibility by their ability to encode large and complex structures representing solutions in a simple form like bit strings for many different applications [25], including multicast routing [26]. GA has been applied to various instances of Steiner tree problems [27] and constrained subgraphs search problems. GA performs well for the Steiner tree problem due to the ability of its operators to combine the good structures of the tree to form better individuals [28]. In constrained subgraph problems, the solution should provide a minimal summation of one or multiple fitness metrics and additionally satisfy one or multiple constraints. GA have the flexibility to tackle all these inputs and evaluate different variants of the problem [29].

GA is implemented based on the *pymoo* library [30], which is a Python-based library tailored for solving multi-objective optimization problems. The implementation of Non-dominated Sorting Genetic Algorithm-II (NSGA-II) algorithm is based on the algorithm version proposed in [31]. The problem is solved on graphs, which are stored and processed by library *NetworkX* [32]. *NetworkX* library is also used to retrieve the number of NDPs for the original graph and the solution candidates based on the maximum flow calculation method.

One of the constraints requires MCF problem to be solved. In this work, MCF problem is formulated as a continuous flow for symmetric multiple-source and multiple-destination commodities of equal size. The complexity of the problem grows according to the network size and amount of the commodities to be forwarded but can be solved by standard solvers [33]. *Gurobi* [34] optimizer is employed to solve the enclosed MCF problem.

C. NSGA-II Procedure

The GA procedure includes chromosome encoding strategy, hyperparameter, and operator selection. Each candidate solution must be represented in a special way suitable for the application and adaptable to the GA. For the given problem, a whole graph structure can be encoded as a chromosome by its nodes or links. Since the edge weights should be evaluated additionally, an edge-based encoding allows access to edge information to the objective function. The initial population is generated randomly based on the original graph encoding. It should also be ensured that the candidate solution is a connected graph, which includes all the access nodes. This selection approach reduces the number of chromosomes passed for further evaluation and reduces the runtime. Next, it should be ensured that all the communication demands are routable by solving MCF problem.

The candidate solution generation and evaluation procedure for GA is presented in Algorithm 1. From each chromosome, a candidate solution is assembled and tested for connectivity, presence of all the terminal nodes, and routability. The fitness of each candidate solution determines the likelihood that it will transfer its genes to potential successors and is evaluated by size-centric and robustness-specific fitness. The size-centric fitness captures the number of edges. The robustness-centric fitness tracks penalty for the missing NDPs in the solution. The solutions are compared by Pareto dominance.

Algorithm 1: Candidate Solution Evaluation

```
/* Ensure original ICT graph is not empty and
   access nodes are present */
Ensure H ≠ ∅, ∃V_H, ω_{V_H} > 0
/* Encode the original graph per edge */
G_encoded ← Encode(G)
/* Create candidate graphs as chromosomes */
Candidates ← CreateChomosomes(G)
/* Evaluate candidates */
foreach Candidate ∈ Candidates do
    /* Create candidate graph from the
       chromosome */
    G_c ← AssembleGraph(Candidate)
    /* Created graph is connected */
    if G_c is connected then
        /* All access nodes are included */
        if ∀V_H, ω_{V_H} > 0 ∈ H : V_H ∈ G_c then
            /* All demands are routable */
            if SolveMCF(G_c) is Feasible then
                /* Find graph size value */
                ObjSize ← Size(G_c)
                /* Find node-disjoint paths
                   penalty value */
                Penalty(G_c) = 1 − (NDP_{G_c}/NDP_G)
                ObjNDP ← Penalty(G_c)
end foreach
return ObjSize, ObjNDP
```

Pymoo library supports various GA operators in the suite of NSGA-II algorithm by Deb et al. [30]. The performance of the operators has been evaluated during the preliminary assessment. Combining binary random sampling, exponential crossover, and bitflip mutation has demonstrated the best and the most stable performance.

V. Evaluation

This section first discusses an appropriate benchmark model for the evaluation. Next, an extensive simulation is performed to demonstrate the robustness of the developed solutions against the ICT nodes being not recoverable for the different network scenarios. Finally, the impact of additional resilience guarantee for the low fraction of priority nodes is investigated.

A. Evaluation Scenarios and Assumptions

This work emphasizes modeling the network's access and backhaul levels during the power system restoration. Therefore, required ICT network benchmarks should include a realistic distribution of these node types. Fundamental benchmark data sets for telecommunications, such as [35], are application-specific and do not represent public cellular networks. On the other hand, topology-based benchmarks, such as [36] and [37], focus on large autonomous systems and do not represent the required network scale. Benchmarks derived from publicly available data on edge cellular networks at the required scale were recently introduced in [38] and could be regarded as illustrations of different edge network configurations.

The MEC benchmark graph [38] with 25 nodes and 50 edges has been selected for evaluation. This graph comprises 21 MEC and 4 (16%) backhaul nodes. It is assumed that a MEC node is an access node with additional edge computing features. Additional graph instances with increased to 64% *(Ing64)* and 80% *(Ing80)* ratios of backhaul nodes were generated to demonstrate the potential dispersion of access nodes and improve the possible number of NDPs between assets. Table I presents the ICT graph parameters of the selected demonstration scenarios. These scenarios are visualized in Figure 3. The density and placement of the access nodes within scenarios were selected to represent the potential interplay between ICT and power system. The power grid and access network infrastructures overlap at the network's edge, while backhaul components enable data forwarding via multiple hops. For the evaluation, 10 power system nodes have been attached to each ICT access node, according to the observations discussed in Section III-A.

One of the objectives of the developed methodology is to guarantee that solutions can route the power system communication demands. MEC benchmark includes reference values, allowing the traffic model's approximation. It is assumed that a distributed optimization algorithm is deployed to restore the power system and uses ModBus UDP protocol messages of 255 bytes for data exchange. Since the benchmark network infrastructure belongs to the public provider [38], the portion of the bandwidth leased by power grid is assumed to be 1 Gbit/s. Therefore, the size of one commodity of power system restoration traffic for the flow calculation is $2 \cdot 10^{-7}$ units.

B. Trade-off between the Restored Network Size and Its Robustness against Node Failures

The scenarios discussed in Section V-A are used to test the Algorithm 1. The algorithm aims to reduce the network size and maximize the number of 2 NDPs between access nodes while ensuring that all the access nodes are present. Figure 4 demonstrates two solutions at the Pareto front for *Ing80* scenario with 5 dispersed access nodes. Table I provides an overview of the solutions and their parameters.

It can be observed that the algorithm has picked near the minimal network size in Figure 4a. The minimum network size would be a minimum Steiner tree connecting all the access nodes. With the presence of the second robustness objective, the algorithm is not enforcing such a tree structure. In Figure 4b, the algorithm aims to select edges to disjoin the node paths for the access nodes. The solution network maintains two edges for each access node, that are not in place for the minimum-size network. In case 2 NDPs do not exist for all the access nodes in the graph structure, the algorithm will seek to find the maximum of possible paths. Since NDP uniqueness is not enforced, the paths can overlap, and the solution network may have a ring topology in which each access node is connected to two backhaul nodes. This may be observed for scenarios with dispersed access nodes, such as in *Ing80* scenario, and be not the case for scenarios with more dense placement of the access node, such as *Ing64*. Uniqueness of NDPs further increases the graph size, the feasibility of such objective will be discussed in future work.

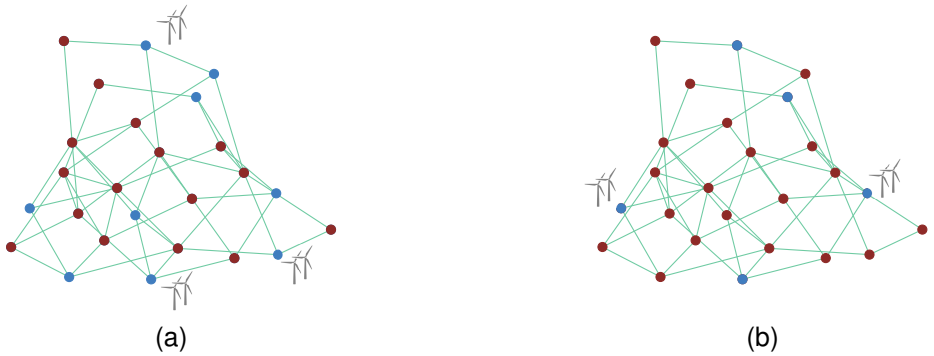

Fig. 3. Examples of generated MEC graph instances for scenarios *Ing64* and *Ing80* with various densities of access nodes (blue) and backhaul nodes (red). (a) Scenario *Ing64* (b) Scenario *Ing80*. Priority access nodes with important power grid components in coverage are marked with a renewable generator icon.

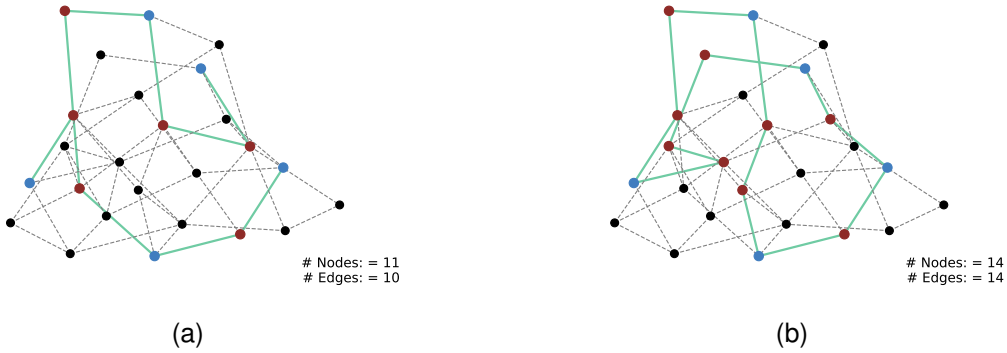

Fig. 4. Resulting Pareto optimal solutions for *Ing80* scenario: MEC graph with 25 nodes and 50 edges, 5 access nodes (blue) and 20 backhaul nodes (red). Included in the solution edges are marked green. Not included in the solution nodes and edges graph are depicted in black. The network size objective dominates in the solution network (a). Path redundancy objective dominates in the solution network (b).

C. Impact of Path Redundancy on Robustness against Node Failures

This section evaluates the impact of considering additional communication paths for access nodes. Extensive simulation of the node failure scenarios is completed to demonstrate the overlay's robustness. In the node failure scenario, a backhaul node can appear unrecoverable during the power system restoration with a given probability. When one or multiple nodes are not recoverable, the ICT network is split into segments $\delta \in \Delta$. A segment δ is not guaranteed to contain all the access nodes and is assumed to be a subnetwork consisting of at least two nodes. This means that part of the power grid in the coverage area of the isolated access node cannot contribute to the power grid restoration.

Depending on the level of robustness expressed as a number of present 2 NDPs or 3 NDPs between all or selected access nodes, the ICT network can tolerate higher failure probabilities without experiencing segmentation. To retrieve solutions with 3 NDPs, the respective objective has been updated in Algorithm 1. Figure 5 shows the impact of the node failure probability on the share of communicating access nodes within the largest segment δ_{max} for the *Ing80* scenario. The minimum-size network (*min-2ndp-all-nodes*) solution's performance decreases drastically at the low probability of

TABLE I
SCENARIO AND SOLUTION GRAPH PARAMETERS

Scenario	$\|V_c\|$	$\|E_c\|$	% Backhaul	|Accces|	|Backhaul|	Solution name	Objectives	$\|V_c\|$	$\|E_c\|$	|Backhaul|
Ing64	25	50	64%	9	16	min-2ndp-all-nodes	size, 2 NDPs	13	12	4
						max-2ndp-for-budg3	size, 2 NDPs for 3 prio	13	13	4
						max-2ndp-all-nodes	size, 2 NDPs	15	16	6
						max-3ndp-all-nodes	size, 3 NDPs	22	28	13
						max-3ndp-for-budg2	size, 2 NDPs, 3 NDPs for 3 prio	20	22	11
Ing80	25	50	80%	5	20	min-2ndp-all-nodes	size, 2 NDPs	11	10	6
						max-2ndp-for-budg2	size, 2 NDP for 2 prio	12	12	7
						max-2ndp-all-nodes	size, 2 NDPs	14	14	9
						max-3ndp-all-nodes	size, 3 NDPs	19	22	14
						max-3ndp-for-budg2	size, 2 NDPs, 3 NDPs for 2 prio	16	16	11

node failure. Solutions with 2 NDPs (*max-2ndp-all-nodes*) and 3 NDPs (*max-3ndp-all-nodes*) can diminish the effect of node failures. For the severe disruptions with $p \geq 0.7$, solutions degrade due to the diffused nature of the access nodes in the scenario. The results suggest that increasing the minimum ICTs network size by 27 % of nodes to guarantee 2 NDPs can improve network robustness for more than 13 % for moderate and more than 10 % for severe failures, respectively. Figure 8 additionally visualizes the number of available paths in each solution and how this number degrades with different probabilities of nodes being not recoverable.

Figure 6 compares minimum size network with 2 and 3 NDPs networks for the *Ing64* scenario. Due to the higher share of access nodes, one can note more radical loss in the minimum-size network performance. For the failure probability of $p = 0.4$, the minimal network is capable of connecting only 58 % of access nodes within δ_{max}, while a robust network with 2 NDPs - 75 % and network with 3 NDPs - 87 %. For $p = 0.6$, the gap between the minimal size and 2 NDPs network is 13 %. At the same time, the network with 2 NDPs requires just 2 (15 %) additional ICT nodes to be picked up. For power grid restoration, a larger value of δ_{max} indicates improved communication capability among power grid components. In the presence of available generation, this facilitates the restoration of larger grid segments by exchanging status and control signals.

One should note that the failure diminishing effect highly depends on the density, level of mesh, and constellation of the access and backhaul nodes for the target scenario. For the intelligent edge networks that support self-backhauling [39], a higher share of the access nodes will be connected in the disrupted network. Scenario *Ing64* illustrates this behavior as it features a portion of access nodes connected via direct links, as shown in Figure 3a. Such clusters ensure that in the worst-case scenario of $p = 1$, a low percentage of the access nodes will be connected in one segment. In the case of *Ing64*, such a segment δ_{max} includes a maximum of two access nodes (22% of 9 access nodes). For the power grid restoration, this provides a basic guarantee that the grid components in such an access cluster will remain connected. This indicates the need to enhance the access nodes' self-backhauling capabilities in practice. Even with the existence of such clusters, the methodology that was developed remains relevant. It can be applied to identify the optimal backhaul structure to connect the clustered access nodes over a wider area.

D. Impact of Path Redundancy on Robustness against Node Failures while Considering Node Priority

This section evaluates the impact of elevating path redundancy for some priority access nodes. An ICT access node priority may depend on the presence of critical for the restoration process power system assets in its coverage, for example, smart inverter-supported battery storage system or larger generation unit. Communication between these assets in the early phase of the power grid restoration may provide detailed insight into available generation, facilitating faster load pick-up. It is, therefore, essential to guarantee that these assets are connected with a higher level of robustness.

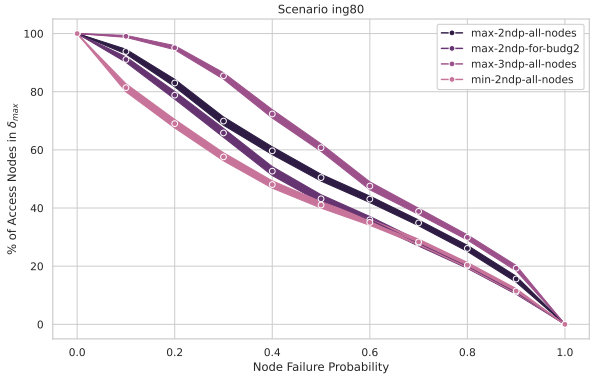

Fig. 5. Percentage of access nodes in largest connected component δ_{max} depending on the probability of a backhaul node not recovering during the restoration for *Ing80* scenario.

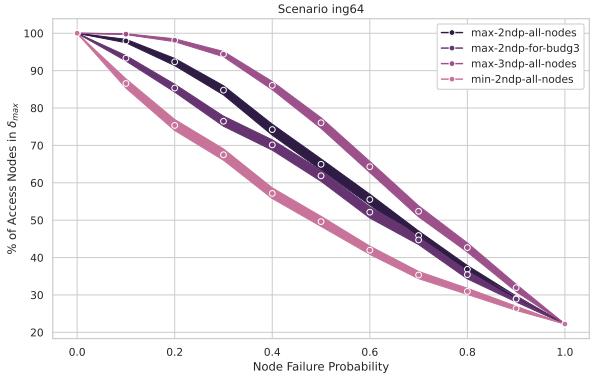

Fig. 6. Percentage of access nodes in largest connected component δ_{max} depending on the probability of a backhaul node not recovering during the restoration for *Ing64* scenario.

1) Including priority assets under limited 2 NDP budget: While 2 and 3 NDPs solutions provide such robustness, experiments in Section V-C show these networks as more expensive in terms of network size and may appear impracticable for the power system restoration. Not all desired ICT loads may be picked up during restoration due to a limited number of switching operations or shortage of generation. This introduces a budget of access nodes for which 2 NDPs can be supported.

A weighted version of the problem in Eq. (7) is introduced to express budget conditions. A weight σ_a is assigned for each power system bus V_{p_a} based on its type, capacity and controllability. An ICT access node V_{C_i} weight ω_i is set by multiplying the number of the power buses in coverage of V_{C_i} by their weights σ. The value of ω also reflects the intensity of the communication, which may be higher for the priority nodes due to the exchange of the signals or pick-up schedules. The penalty function in Eq. (2) is updated to maximize the weight of the nodes connected with 2 NDPs under the given budget.

The results for *Ing64* scenario are presented in Figure 6. The curve *max-2ndp-for-budg3* demonstrates the solution that provides 2 NDPs for a budget of 3 nodes. The algorithm has selected the nodes with the highest weight, marked in Figure 3a. The solution differs by only one extra edge (see Table I). Yet, it demonstrates a notably better failure diminishing effect

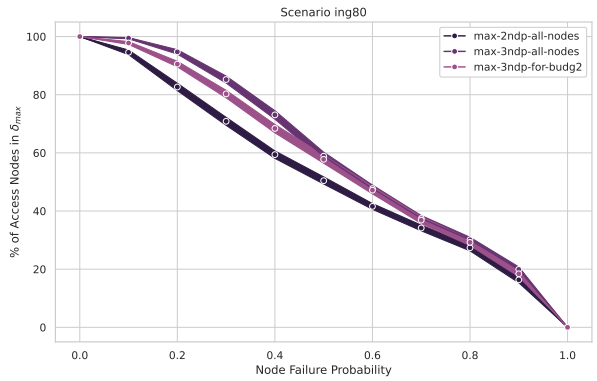

Fig. 7. Percentage of access nodes in largest connected component δ_{max} depending on the probability of a backhaul node not recovering during the restoration for *Ing80* scenario, considering the budget of 3 NDPs for 2 nodes.

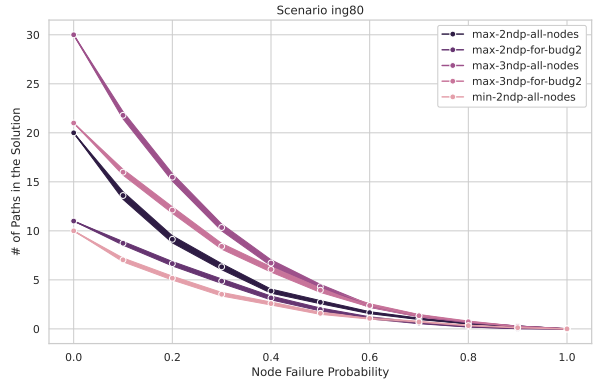

Fig. 8. Number of paths between the pairs of access nodes in the solution depending on the probability of a backhaul node not recovering during the restoration for *Ing80* scenario.

than a minimal network with 78 % of access nodes in δ_{max} for $p = 0.3$. In contrast, the minimal network only has 65 % of access nodes. Compared with the solution with all 2 NDPs (*max-2ndp-all-nodes*), the partial solution provides about 6 % less robustness till $p \leq 0.5$. The partial solution has a higher total of 2 NDPs than the minimum size graph. Therefore, its performance degrades similarly to the solution with 2 NDPs between all access nodes and merges with it by $p \geq 0.8$ when both networks reach a similar number of paths.

A partial solution for the high-priority nodes has also been tested for *Ing80* scenario for a budget of 2 priority nodes, marked in Figure 3b. The solution that only provides 2 NDPs between the selected two priority nodes (*max-2ndp-for-budg2*) initially enhances robustness but then quickly deteriorates to the performance of the minimal network. Robustness improvement of 5 % for $p \leq 0.3$ costs 1 additional ICT load. Figure 8 demonstrates the degradation of solutions regarding available paths. For power grid restoration, these results suggest that even with a restricted budget for robustness, ICT networks can be found with higher performance than a minimal-sized network while maintaining a compact size and guaranteeing robust communication between important grid assets.

2) Including priority assets under limited 3 NDP budget: A budget can also be introduced when selecting the number of 3 NDPs for the target network. Figure 7 presents the obtained results for the *Ing80* scenario and compares solutions that guarantee 2 and 3 NDPs with a solution that guarantees 3 NDPs for priority nodes and 2 NDPs for the rest of access nodes *max-3ndp-for-budg2*. The results suggest that while the 3 NDPs network provides expectantly the highest robustness, *max-3ndp-for-budg2* solution delivers a significant improvement compared to the 2 NDPs network. The failure diminishing effect of the *max-3ndp-for-budg2* solution is 10 % higher for $p = 0.4$ and $p = 0.5$ for just 2 additional backhaul ICT nodes to be restored. This solution is, at the same time, considerably smaller than the complete 3 NDPs network, offering a viable trade-off between robustness and the actions required from the power grid to pick up additional ICT loads. Therefore, prioritization of ICT access nodes based on their connections to important power grid assets enables the identification of feasible solutions that offer sufficient robustness without being overly extensive.

It is also evident that a higher mesh level enables the forming of node-disjoint paths. However, due to the lack of available provider-approved cellular network benchmark models, a relatively low mesh level and a hierarchical ordering in access and backhaul networks may be observed [22], [38]. Such network structures significantly limit possible efforts to create compact, robust networks for effective power grid restoration, and they should be upgraded to be used for power grid communications.

VI. Conclusion

This work discusses the multi-objective problem of finding a minimum-size robust ICT network to enable communication between the distributed energy resources while restoring the power distribution grid. To assemble such ICT network, a GA-based method is proposed. The method can handle conflicting objectives and constraints, such as reduced network size, increased robustness, routability, and connectivity. The proposed interconnected system model captures dependencies between the ICT and power system, creating a realistic representation of the edge public cellular network.

Post-blackout ICT systems may be severely degraded and susceptible to unexpected behavior. The robustness of designed networks was evaluated under the varying probability of an ICT node being unrecoverable. The results suggest that an optimal ICT network for the power grid restoration can diminish the effect of node failures and keep the access nodes within the same connected segment even by a higher level of disruption. Extreme robustness requirements lead to a large ICT network that may be infeasible to pick up during the restoration. However, a trade-off between the robustness and the network size can be found. The results show that adding a few nodes and edges to the minimum-size network can significantly improve robustness, e.g., between ICT nodes connecting important power grid assets. Meshed, self-backhauling edge networks may further improve the quality of solutions.

The developed methodology is applicable and will be tested with other communication technologies in future work. Limiting factors of currently deployed public and emerging dedicated cellular networks for critical infrastructures regarding the

forming of the optimal ICT networks for emergency scenarios will be evaluated. However, the lack of the available realistic ICT network benchmark models remains a challenge.

ACKNOWLEDGMENTS

This work was funded by the DFG (German Research Foundation), project number 360475113, as part of the priority program DFG SPP 1984 - Hybrid and Multimodal Energy Systems: System theory methods for the transformation and operation of complex networks. A. Ghasemi acknowledges funding from the Alexander von Humboldt Foundation (Ref. 3.4 - IRN - 1214645 - GF-E) for his visiting research at the University of Passau in Germany.

REFERENCES

[1] M. Braun, J. Brombach, C. Hachmann, D. Lafferte, A. Klingmann, W. Heckmann, F. Welck, D. Lohmeier, and H. Becker, "The future of power system restoration: Using distributed energy resources as a force to get back online," *IEEE Power and Energy Magazine*, vol. 16, no. 6, pp. 30–41, 2018.

[2] S. Stark, A. Volkova, S. Lehnhoff, and H. de Meer, "Why your power system restoration does not work and what the ict system can do about it," in *Proc. of the 12th ACM international conference on future energy systems*, 2021, pp. 269–273.

[3] P. Danner, A. Volkova, and H. De Meer, "Two-step blackout mitigation by flexibility-enabled microgrid islanding," in *Proceedings of the 15th ACM International Conference on Future and Sustainable Energy Systems*, ser. e-Energy '24. New York, NY, USA: Association for Computing Machinery, 2024, p. 596–605.

[4] J. P. Sterbenz, D. Hutchison, E. K. Çetinkaya, A. Jabbar, J. P. Rohrer, M. Schöller, and P. Smith, "Resilience and survivability in communication networks: Strategies, principles, and survey of disciplines," *Computer Networks*, vol. 54, no. 8, pp. 1245–1265, 2010, resilient and Survivable networks.

[5] A. Ghasemi and H. de Meer, "Robustness of interdependent power grid and communication networks to cascading failures," *IEEE Trans. on Network Science and Engineering*, vol. 10, no. 4, pp. 1919–1930, 2023.

[6] E. Rokrok, M. Shafie-khah, P. Siano, and J. P. Catalão, "A decentralized multi-agent-based approach for low voltage microgrid restoration," *Energies*, vol. 10, no. 10, p. 1491, 2017.

[7] A. Sharma, D. Srinivasan, and A. Trivedi, "A decentralized multi-agent approach for service restoration in uncertain environment," *IEEE Trans. on Smart Grid*, vol. 9, no. 4, pp. 3394–3405, 2016.

[8] L. Yang, Y. Xu, H. Sun, M. Chow, and J. Zhou, "A multiagent system based optimal load restoration strategy in distribution systems," *Int. Journal of Electrical Power & Energy Systems*, vol. 124, p. 106314, 2021.

[9] P. McKeever, E. De Din, A. Sadu, and A. Monti, "Mas for automated black start of multi-microgrids," in *2017 IEEE SmartGridComm*, 2017, pp. 32–37.

[10] J. Wang, C. Qiao, and H. Yu, "On progressive network recovery after a major disruption," in *2011 Proceedings IEEE INFOCOM*. IEEE, 2011, pp. 1925–1933.

[11] N. Bartolini, S. Ciavarella, T. F. La Porta, and S. Silvestri, "Network recovery after massive failures," in *2016 46th Annual IEEE/IFIP International Conference on Dependable Systems and Networks*. IEEE, 2016, pp. 97–108.

[12] D. Z. Tootaghaj, N. Bartolini, H. Khamfroush, and T. La Porta, "On progressive network recovery from massive failures under uncertainty," *IEEE Trans. on Network and Service Management*, vol. 16, no. 1, pp. 113–126, 2018.

[13] D. Z. Tootaghaj, N. Bartolini, H. Khamfroush, T. He, N. R. Chaudhuri, and T. La Porta, "Mitigation and recovery from cascading failures in interdependent networks under uncertainty," *IEEE Trans. on Control of Network Systems*, vol. 6, no. 2, pp. 501–514, 2018.

[14] R. H. Lasseter, Z. Chen, and D. Pattabiraman, "Grid-forming inverters: A critical asset for the power grid," *IEEE Journal of Emerging and Selected Topics in Power Electronics*, vol. 8, no. 2, pp. 925–935, 2020.

[15] T. Vandoorn, J. De Kooning, B. Meersman, and L. Vandevelde, "Review of primary control strategies for islanded microgrids with power-electronic interfaces," *Renewable and Sustainable Energy Reviews*, vol. 19, pp. 613–628, 2013.

[16] Y. Du, H. Tu, X. Lu, J. Wang, and S. Lukic, "Black-start and service restoration in resilient distribution systems with dynamic microgrids," *IEEE Journal of Emerging and Selected Topics in Power Electronics*, vol. 10, no. 4, pp. 3975–3986, 2022.

[17] Y. Han, K. Zhang, H. Li, E. A. A. Coelho, and J. M. Guerrero, "Mas-based distributed coordinated control and optimization in microgrid and microgrid clusters: A comprehensive overview," *IEEE Trans. on Power Electronics*, vol. 33, no. 8, pp. 6488–6508, 2018.

[18] S. Meinecke, D. Sarajlić, S. R. Drauz, A. Klettke, L.-P. Lauven, C. Rehtanz, A. Moser, and M. Braun, "Simbench—a benchmark dataset of electric power systems to compare innovative solutions based on power flow analysis," *Energies*, vol. 13, no. 12, 2020.

[19] M. Wissner, B. Sörries, and W. Zander, "The 450 mhz frequency as a forerunner of the energy transition," *Zeitschrift für Energiewirtschaft*, vol. 44, pp. 163–175, 2020.

[20] CIGRE Study Committee C6, "Benchmark systems for network integration of renewable and distributed energy resources," Tech. Rep., jan 2014, [Accessed: 20 March 2024].

[21] A. Volkova, J. Terzer, and H. de Meer, "Quantifying geospatial interdependencies of ict and power system based on open data," *Energy Informatics*, vol. 4, pp. 1–12, 2021.

[22] M. Zhou, B. Li, M. Yang, and L. Pan, "Telegraph: A benchmark dataset for hierarchical link prediction," *arXiv preprint arXiv:2204.07703*, 2022.

[23] J. W. Suurballe, "Disjoint paths in a network," *Networks*, vol. 4, no. 2, pp. 125–145, 1974.

[24] K. Salimifard and S. Bigharaz, "The multicommodity network flow problem: state of the art classification, applications, and solution methods," *Operational Research*, pp. 1–47, 2022.

[25] G. E. Liepins and M. Hilliard, "Genetic algorithms: Foundations and applications," *Annals of operations research*, vol. 21, no. 1, pp. 31–57, 1989.

[26] G. Zhou, M. Gen, and T. Wu, "A new approach to the degree-constrained minimum spanning tree problem using genetic algorithm," in *1996 IEEE Int. Conf. on Systems, Man and Cybernetics. Information Intelligence and Systems*, vol. 4, 1996, pp. 2683–2688 vol.4.

[27] A. Kapsalis, V. Raywad-Smith, and G. D. Smith, "Solving the graphical steiner tree problem using genetic algorithms," *Journal of the Operational Research Society*, vol. 44, no. 4, pp. 397–406, 1993.

[28] J. Hesser, R. Männer, and O. Stucky, "On steiner trees and genetic algorithms," in *Parallelism, Learning, Evolution*, J. D. Becker, I. Eisele, and F. W. Mündemann, Eds. Berlin, Heidelberg: Springer Berlin Heidelberg, 1991, pp. 509–525.

[29] Q. Zhang, S. Yang, M. Liu, J. Liu, and L. Jiang, "A new crossover mechanism for genetic algorithms for steiner tree optimization," *IEEE Trans. on Cybernetics*, vol. 52, no. 5, pp. 3147–3158, 2022.

[30] J. Blank and K. Deb, "Pymoo: Multi-objective optimization in python," *IEEE Access*, vol. 8, pp. 89 497–89 509, 2020.

[31] K. Deb, A. Pratap, S. Agarwal, and T. Meyarivan, "A fast and elitist multiobjective genetic algorithm: Nsga-ii," *IEEE Trans. on Evolutionary Computation*, vol. 6, no. 2, pp. 182–197, 2002.

[32] A. Hagberg, P. Swart, and D. S Chult, "Exploring network structure, dynamics, and function using networkx," Los Alamos National Lab, Los Alamos, NM, US, Tech. Rep., 2008.

[33] D. Weibin, J. Zhang, and S. Xiaoqian, "On solving multi-commodity flow problems: An experimental evaluation," *Chinese Journal of Aeronautics*, vol. 30, no. 4, pp. 1481–1492, 2017.

[34] Gurobi Optimization, LLC, *Gurobi Optimizer Reference Manual*, 2024, [Accessed: 24 March 2024]. [Online]. Available: https://www.gurobi.com

[35] S. Orlowski, R. Wessäly, M. Pióro, and A. Tomaszewski, "Sndlib 1.0—survivable network design library," *Networks: An International Journal*, vol. 55, no. 3, pp. 276–286, 2010.

[36] S. Knight, H. X. Nguyen, N. Falkner, R. Bowden, and M. Roughan, "The internet topology zoo," *IEEE Journal on Selected Areas in Communications*, vol. 29, no. 9, pp. 1765–1775, 2011.

[37] B. Zhang, R. Liu, D. Massey, and L. Zhang, "Collecting the internet as-level topology," *SIGCOMM Comput. Commun. Rev.*, vol. 35, no. 1, p. 53–61, jan 2005.

[38] B. Xiang, J. Elias, F. Martignon, and E. Di Nitto, "A dataset for mobile edge computing network topologies," *Data in Brief*, vol. 39, p. 107557, 2021.

[39] R. Favraud, C.-Y. Chang, and N. Nikaein, "Autonomous self-backhauled lte mesh network with qos guarantee," *IEEE Access*, vol. 6, pp. 4083–4117, 2018.